

# An Efficient MPPT Technique Using MIASO Based NARMA-L2 Controller for SPV Generator

Sunita Chahar\*<sup>‡</sup> , D. K. Yadav\*\* 

\* Department of Electrical Engineering, Rajasthan Technical University Kota, Rajasthan (India)

\*\* Department of Electrical Engineering, Rajasthan Technical University Kota, Rajasthan (India)

(schahar@rtu.ac.in, dkyadav@rtu.ac.in)

<sup>‡</sup> Sunita Chahar; Research Scholar, Department of Electrical Engineering, Rajasthan Technical University Kota, Rajasthan

Tel: +919462832662, schahar@rtu.ac.in

*Received: 01.07.2021 Accepted: 27.07.2021*

**Abstract-** This paper describes an efficient solution to make a solar photovoltaic (SPV) generator more promising and acceptable to generate continuous power over the different inherent and extraneous unpredictable factors. A significant problem of the SPV generators is to harness optimal power and its complicated nonlinear power-voltage characteristics with multiple sags swells under shedding conditions and dynamic insolation patterns. A novel state-of-the-art technique of maximum power point tracking (MPPT) using multi-input and single-output (MIASO) based nonlinear autoregressive moving average controller (NARMA-L2) is used. It is employed to govern two inputs of two SPV generators by controlling one output duty cycle of one boost converter to take out continuous maximum power under macro and micro-dynamic environmental data. It can adjust power supply according to demand under the same or different insolation pattern. One of the strongest reasons to use this technique is to improve the system's performance to the next level of perfection as it can easily be able to differentiate the global point of maximum power (GPMP) and local point of maximum power (LPMP). Its efficient control capability with a large no of a database is showing its proficiency in uncertain nonlinear environmental conditions, and controllability of separate controllers for each SPV generator. In this paper, the post-performance in terms of least MSE (Mean Square Error) and the maximum efficiency is enhanced up to 98.15%, and 97 % for macro and micro environmental data respectively. The MATLAB simulation results of the SPV generator configuration with the proposed novel MPPT technique are found superior.

**Keywords** MIASO, NARMA-L2, MPPT, FFMNN, SPV, MSE.

## Nomenclature

|                     |  |
|---------------------|--|
| MPPT                | Maximum Power Point Tracking                       |
| LPMP                | Local Point of Maximum Power                       |
| GPMP                | Global Point of Maximum Power                      |
| SPV                 | Solar Photo Voltaic                                |
| PV                  | Photovoltaic                                       |
| MIASO               | Multi-Input And Single Output                      |
| NARMA-L2            | Nonlinear Autoregressive Moving Average Controller |
| ANN                 | Artificial Neural Network                          |
| PV <sub>syst</sub>  | PVsyst Simulation Software                         |
| I <sub>source</sub> | Source Current, Amps                               |
| I <sub>d</sub>      | Reverse Saturation Diode Current, Amps             |
| V <sub>d</sub>      | Voltage Across Diode, Volt                         |
| R <sub>p</sub>      | Parallel Resistance, Ohm                           |

|            |  |
|------------|--|
| $I_{pv}$   | Current Across PV Solar, Amps            |
| q          | Absolute Value of e-Charge, Coulomb      |
| N          | Ideality Factor                          |
| K          | Boltzmann's Constant, J/K                |
| T          | Absolute Temperature, °C                 |
| $V_{pv}$   | Generated Voltage in SPV Generator, Volt |
| $R_{se}$   | Series Resistance, Ohm                   |
| FFMNN      | Feed Forward Multi Neural Network        |
| d1& d2     | Baise Signals                            |
| $V_{ip}$   | Inputs Voltage, Volt                     |
| $V_{op}$   | Output Voltages, Volt                    |
| $I_{op}$   | Output Current, Amps                     |
| $\Delta V$ | Ripples in Voltage                       |
| $\Delta I$ | Ripples in Current, Amps                 |
| $f_{sw}$   | Switching Frequency, Hz                  |
| L          | Inductance, Henry                        |
| C          | Capacitance , Farads                     |
| SAM        | System Advisor Model                     |
| NREL       | National Renewable Energy Laboratory     |
| DR         | Duty Ratio                               |

## 1. Introduction

Sustainable development goal 13 of the 17 goals is the action needed for Climate Change. With the increase of population and new technological advancement, there is an increase in the requirement of energy in the recent past [1]. Earlier most of the electricity was produced by conventional energy sources. Due to unfavorable issues of conventional energy sources like the adverse effect of greenhouse gas, costly maintenance, restrictions of installation sites, and selection of a site, it is required to use clean and environment-friendly source of energy. In contrary to established conventional types of energy sources, the power generation from various types of renewable energy sources has a leading role to mark a new epoch to constitute sustainable energy in the power system [2]. The worldwide average consumption of nonconventional energy increased at the rate of 2% every year from 2008 to 2018 [3].

The meteoric growth in energy requirement forced us to fulfill the power demand based on availability over the wide area, efficacy, and invulnerability criteria for the populace. Thus different types of renewable energy sources provide the required feasibility of sustainable generation as per consumer's needs. There are different types of REGS (renewable energy generation sources) ocean wave energy, wind energy, biomass energy, solar energy, and geothermal energy system, etc [4].

Out of different REGS, solar energy source has been flashed as trending and leading renewable sources as it is solely and in combination with other types of REG is found cost-effective and efficacious. In the past two decades, many research on SPV generators has been conducted as an important nonconventional energy source because it is inexhaustible, abundant, and clean REGS [5-7]. SPV generators can produce electrical energy from solar

irradiance through a solar PV panel. The conversion efficiency of the SPV generator is 15-22% which indicates that it can change 1/6 to 1/5 part of solar energy into electrical energy [8]. The power output from SPV generator is directly affected by the episodically and unpredictable environmental conditions. As a result, this is one of the key issues to get power and enhance conversion efficiency with varying solar irradiance and temperature. SPV generators situated at the site can experience many geographical factors like dust deposition, cloudy weather, building sheds and so many reasons to project irregular shadows on the PV solar panel's surface thus there are multiple sag and swells on the PV curve. Therefore this is another issue that makes PV characteristics more complex [9].

## 2. Related Survey

To investigate and review the work related to MPPT techniques, ANN and MIAISO for SPV generator has been done in this section. In this context to obtain maximum possible power from SPV generator, to control tracking efficiently, proper tracing of the global point of maximum power on PV curve many research fellows explored the performance of PV solar modules and different tracking control strategies. There are more than 50 different MPPT techniques and approximately tens of thousands of publications on control techniques available in the literature for photovoltaic applications. All these are categorized into four groups as conventional tracking schemes, novel tracking schemes, hybrid tracking schemes, and modified hybrid tracking schemes. The conventional tracking schemes are easy to contrive however they may not be able to differentiate between LPMP and GPMP and tracking speed is also slow. Novel tracking schemes and hybrid tracking schemes are better in accuracy but need tricky computation and again associated with the similar problem of uncertainty in tracking GPMP from multi peaks under

dynamic insolation patterns. Modified hybrid tracking scheme has a specialty of more accuracy but needs efficient computational skills and costly realization. However, to optimize the SPV generator this is difficult to choose a particular control technique from so many of the techniques available in the research domain as every process has its pros and cons [10-22].

In the present scenario, the automation environment leads us to deal with time-bound problems. In this context, many researchers prefer artificial neural network (ANN) in SPV generator as it offers better tracking speed, reduced power oscillation, and efficient performance over the previous demerits of other MPPT techniques [23-28]. Day by day it draws the attention of researchers because of its proficiency and demonstrates a superior performance with inherent and extraneous factors. One of the strongest reasons that enforce the author to use the ANN-based controlling technique is their excellent capability to model with aforementioned nonlinearity, complex characteristics, and uncertainties, and in addition their not dependency on appropriate mathematical implementation of SPV generator. This will be a more acceptable renewable energy source if we found judicious controllability of key issues like better efficiency, better controllability to produce maximum power, and better performance under shedding conditions for that reason author has proposed a technique to integrate multi-input single output with an MPPT scheme to get aforementioned objectives in the SPV generator. Numerous research works are conducted related to multi-input and multi-output. However, very few works have been proposed related to multi-input and single output in literature [29-31].

In this paper, the author presents a novel MPPT technique using MIASO based NARMA-L2 controller. In this context, the following contribution is developed for SPV generator configuration, and performance is proved by post evaluation and simulation results under micro and macro environmental variables:

1. Novel MPPT technique using MIASO based NARMA-L2 controller for two SPV generators with one boost converter.
2. Design MIASO based NARMA-L2 controller using mathematical equations.

**3. System Design of a PV Array**

A PV solar system consists of an array of series, parallel possible combinations of PV modules to get desired output voltage, current, and power capacity. The rated value of voltage and power of a SPV cell is 0.35 volt -0.45 volt, 1-2 W respectively. This varies according to the material used and the surface area [7]. Fig.1 is showing the circuit diagram of one cell of SPV generator [32]. And the mathematical formulation of the generated voltage in SPV generator is represented by the following Eq. (1) – (3). Source current  $I_{source}$  varies according to solar irradiation. Applying KCL (Kirchhoff current law) on two resistance equivalent models of SPV. We get the current equation of one cell of SPV generator –

$$I_{source} - I_d - V_d/R_p - I_{pv} = 0 \tag{1}$$

Diode current  $I_d$  is the total current through diode due to activated electrons and holes presented by Eq. (2).

$$I_d = I_s (e^{(qV_d / NKT)} - 1) \tag{2}$$

The generated voltage  $V_{pv}$  is shown in Eq. (3), when the load is connected at the output terminal. It is equal to the difference of diode voltage ( $V_d$ ) and the voltage drop across series resistance.

$$V_{pv} = V_d - R_{se} I_{pv} \tag{3}$$

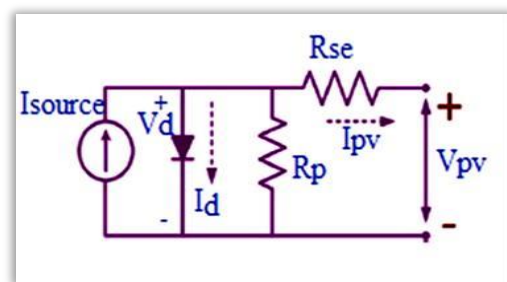


**Fig.1** Circuit diagram of one cell of SPV generator

Here  $q$  is the  $e^-$  charge and it has a standard value i.e.  $1.6 \times 10^{-19}$  C. And  $K$  is Boltzmann’s constant and has a standard value i.e.  $1.38 \times 10^{-23}$  J/K.

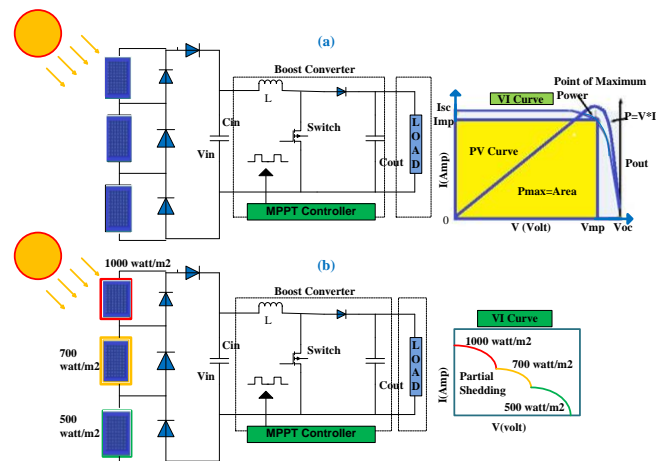


**Fig.2(a)** SPV generator with MPPT controller and its nonlinear characteristics and **Fig.2 (b)** SPV generator with MPPT controller and its nonlinear characteristics under partial shedding condition

Figure 2(a) is showing a SPV generator with an MPPT controller and its nonlinear characteristics. And Fig.2(b) is representing a SPV generator with an MPPT controller under the partial shedding condition resulting in many peaks and corresponding complex nonlinear characteristics.

**4. Proposed Methodology**

*4.1 Description of the MPPT technique using MIASO based NARMA-L2 Controller*

Here inputs of two SPV generators are controlled by two NARMA-L2 controllers and one output signal is given to the switch in the boost converter. Therefore maximum power output from two SPV generators can extract. And continues power flows to the load if one SPV generator is disconnected. NARMA-L2 is a remarkable neural network structure for precise tracking and efficient input to output restrain. This controlling process gives direction for linearization of desired SPV generator’s output pattern where this is an affine function of two updated signals from output [28].

This adopts the following actions:

- 4.1.1 The identification process of SPV generator
- 4.1.2 Control design process

*4.1.1 The identification Process of SPV generator*

In this process, we train a neural network. Parameters used by the author for the identification process are mentioned in Table 1.

**Table 1.** Parameters used in identification process

| Dataset Parameters         | Dataset-I        | Dataset-II       | Dataset-III      | Dataset-IV       | Dataset-V        |
|----------------------------|------------------|------------------|------------------|------------------|------------------|
| Size of the Hidden Layer   | 5                | 3                | 3                | 3                | 5                |
| Delayed Controller Outputs | 1                | 1                | 1                | 1                | 1                |
| Delayed Plant Outputs      | 1                | 1                | 1                | 1                | 1                |
| Sampling Interval          | 0.01             | 0.01             | 0.01             | 0.01             | 0.01             |
| Generate Training Data     | 10910            | 246              | 100              | 31               | 981              |
| Training Epochs            | 300              | 300              | 300              | 300              | 300              |
| Validation                 | 20 % of data set | 20 % of data set | 20 % of data set | 20 % of data set | 20 % of data set |
| Testing                    | 20 % of data set | 20 % of data set | 20 % of data set | 20 % of data set | 20 % of data set |

From Table 1. the total no of samples of datasets are divided into three sets of the sample which is arbitrarily picked by neural network tool. Out of which, 60% samples are used for training of the network, 20% for validation, and the rest 20% for testing. Testing Samples are used to find MSE. Validation samples are used for the network to make it familiar with the pattern.

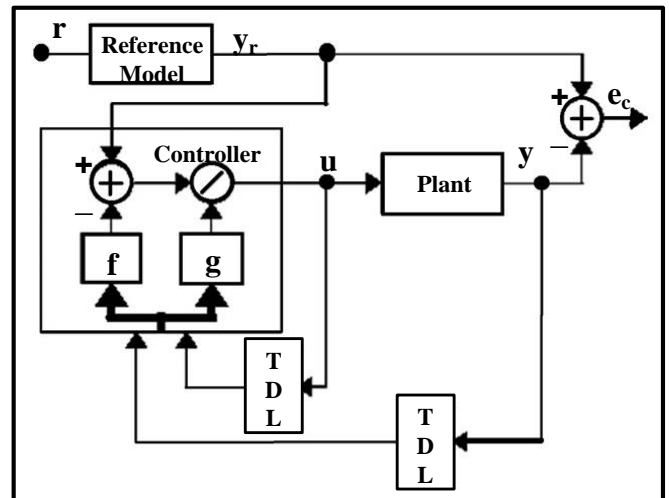


**Fig.3** Block diagram of standard NARMA-L2 controller with FFMNN

The biases and weight are reorganized. Then set to a new value in each iteration according to the output from plant and sample pattern used for SPV generator.

The NARMA-L2 approximate configuration has two f and g FFMNN as shown in Fig.3. With the help of these SPV generators are recognized by the controller [34-35]. The system equation is-

$$\hat{y}(t-1) = f \left[ y(t), y(t-1), \dots, y(t-n+1), u(t-1), \dots, u(t-p+1) \right] + g \left[ y(t), y(t-1), \dots, y(t-n+1), u(t-1), \dots, u(t-p+1) \right] \times u(t-1) \tag{4}$$

Here p and q are indicating previous output and input numbers.

*4.1.2 Controller Design Process*

Two FFMNN are used. This is represented by fnn and gnn. In the authors' configuration, each one is a feed-forward with 3, 3, 3, 5, and 5 layers for five datasets. Three layers are consist of an input, a hidden and an outermost layer. Five layers are consist of an input, three intermediate, and an outermost layer. The input layer of the fnn FFMNN has two nodes. One is output power and the second one is

d1, d2 bias signals. The input layer of the gnn FFMNN has two nodes for the duty ratio and d1, d2 bias signal. There are three intermediate nodes of the hidden layer. The outermost layer has only one node for each of the two systems and then one DR (duty ratio) output node. The outgoing signal represents the DR signal for the point of maxima on the curve.

To design a NARMA-L2 controller the controlling signal can be generated by using Eq. (4) [33].

$$u_{(t1)} = \frac{y_{(t1-d1)} - fnn \begin{bmatrix} y_{(t1)}, y_{(t1-1)}, \dots, y_{(t1-p+1)} \\ u_{(t1)}, u_{(t1-1)}, \dots, u_{(t1-q+1)} \end{bmatrix}}{gnn \begin{bmatrix} y_{(t1)}, y_{(t1-1)}, \dots, y_{(t1-p+1)} \\ u_{(t1)}, u_{(t1-1)}, \dots, u_{(t1-q+1)} \end{bmatrix}} \quad (5)$$

$$u_{(t2)} = \frac{y_{(t2-d2)} - fnn \begin{bmatrix} y_{(t2)}, y_{(t2-1)}, \dots, y_{(t2-p+1)} \\ u_{(t2)}, u_{(t2-1)}, \dots, u_{(t2-q+1)} \end{bmatrix}}{gnn \begin{bmatrix} y_{(t2)}, y_{(t2-1)}, \dots, y_{(t2-p+1)} \\ u_{(t2)}, u_{(t2-1)}, \dots, u_{(t2-q+1)} \end{bmatrix}} \quad (6)$$

We set  $y_{(t1+d1)} = y_{(t1+d1)}^{ref}$  and  $y_{(t2+d2)} = y_{(t2+d2)}^{ref}$  to follow the base trajectory  $y_{(t1+d1)}^{ref}$  and  $y_{(t2+d2)}^{ref}$  respectively. Therefore our output of the system  $y_{(t1+d1)}$  and  $y_{(t2+d2)}$  is following as per teaching. Put these new values to the designed NARMA-L2 in Eq. (5) and Eq. (6). Then the rearranging output of the controller:

$$u_{(t1)} = \frac{y_{(t1-d1)}^{ref} - fnn \begin{bmatrix} y_{(t1)}, y_{(t1-1)}, \dots, y_{(t1-p+1)} \\ u_{(t1)}, u_{(t1-1)}, \dots, u_{(t1-q+1)} \end{bmatrix}}{gnn \begin{bmatrix} y_{(t1)}, y_{(t1-1)}, \dots, y_{(t1-p+1)} \\ u_{(t1)}, u_{(t1-1)}, \dots, u_{(t1-q+1)} \end{bmatrix}} \quad (7)$$

$$u_{(t2)} = \frac{y_{(t2-d2)}^{ref} - fnn \begin{bmatrix} y_{(t2)}, y_{(t2-1)}, \dots, y_{(t2-p+1)} \\ u_{(t2)}, u_{(t2-1)}, \dots, u_{(t2-q+1)} \end{bmatrix}}{gnn \begin{bmatrix} y_{(t2)}, y_{(t2-1)}, \dots, y_{(t2-p+1)} \\ u_{(t2)}, u_{(t2-1)}, \dots, u_{(t2-q+1)} \end{bmatrix}} \quad (8)$$

$$u_{(t)} = u_{(t1)} + u_{(t2-d2)} \quad (9)$$

$$u_{(t)} = \left\{ \frac{y_{(t1-d1)}^{ref} - fnn \begin{bmatrix} y_{(t1)}, y_{(t1-1)}, \dots, y_{(t1-p+1)} \\ u_{(t1)}, u_{(t1-1)}, \dots, u_{(t1-q+1)} \end{bmatrix}}{gnn \begin{bmatrix} y_{(t1)}, y_{(t1-1)}, \dots, y_{(t1-p+1)} \\ u_{(t1)}, u_{(t1-1)}, \dots, u_{(t1-q+1)} \end{bmatrix}} + \frac{y_{(t2+d2)}^{ref} - fnn \begin{bmatrix} y_{(t2-d2)}, y_{(t2-d2-1)}, \dots, y_{(t2-d2-p+1)} \\ u_{(t2-d2-1)}, \dots, u_{(t2-d2-q+1)} \end{bmatrix}}{gnn \begin{bmatrix} y_{(t2-d2)}, y_{(t2-d2-1)}, \dots, y_{(t2-d2-p+1)} \\ u_{(t2-d2)}, u_{(t2-d2-1)}, \dots, u_{(t2-d2-q+1)} \end{bmatrix}} \right\} \quad (10)$$

Equation (7) to (10) is showing a rearrangement of the control signal for the MIASO based NARMA-L2 controller to approximate SPV generator configuration.

#### 4.2 The Procedure of Controller's Functioning-

The training procedure telecast results are based on MSE at minima. During the training process, our aim is to train both the controllers with the previous desired value as a mimic. It is a teaching process for the controllers and both the controller learns how to behave efficiently for expected output. In this procedure, an error signal is generated if there is a difference between the output of the plant and desired output. In each iteration, the error actuates a controlling signal to produce steps for corrective actions of the neuron's weight and baise. And this loop of corrective settlement is continued until the training data attains the desired pattern to get the target response within close range with less chattering as possible. After some iteration, the controller is well trained and the currently generated weights are stored.

The prime objective of the presented methodology is to trace two inputs that may be the same or of a different pattern. After that continuous maximum possible generation of two SPV generators is provided to the connected load. This is followed by a setting of the suitable duty ratio for both SPV generators at the delay which serves solution to the following main issues:

1. Able to produce the maximum power output.
2. Better control over macro and micro-environmental data.
3. Gives power output without any confusion of local maximum power value at the local dip in the curve in case of shedding.
4. Continues power supply to load at variable insolation pattern.

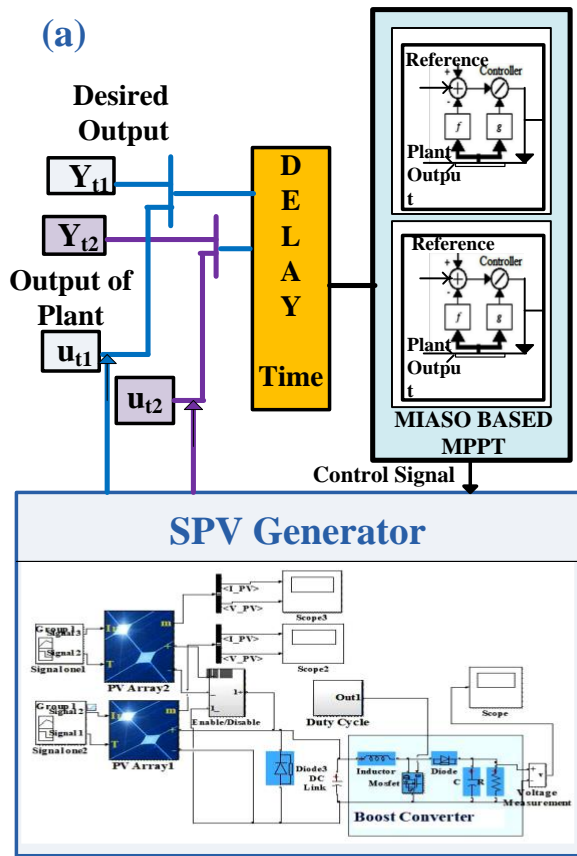


Fig.4(a) Block diagram of the MPPT technique using MIASO based NARMA-L2 controller

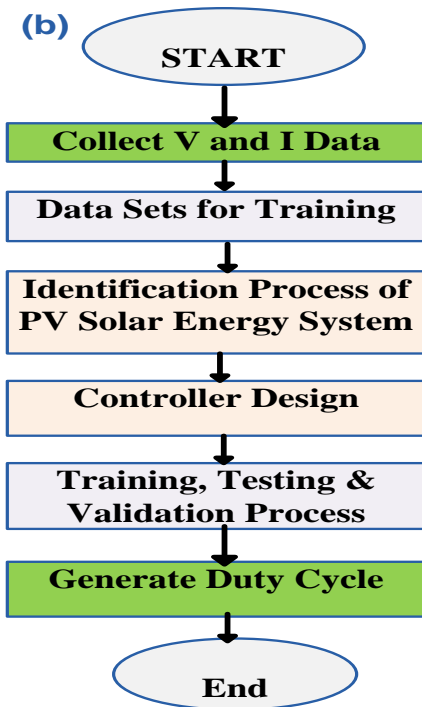


Fig.4(b) Flow chart of MPPT technique using NARMA-L2 controller

The block diagram of the proposed MPPT technique using MIASO based NARMA-L2 controller for SPV generator is presented in Fig.4(a) and the flow chart of the proposed technique is presented in Fig.4(b).

The Proposed controller generates controlling signal DR which is presented by following Eq. (11).

$$DR(t) = \left\{ \begin{array}{l} \text{ref-fnn} \left[ \begin{array}{l} P_{pv(t+d1)} \\ P_{pv(t-p+1)} \\ \dots \\ DR(t-1) \dots DR(t-q+1) \end{array} \right] \\ \text{gnn} \left[ \begin{array}{l} P_{pv(t)} \\ P_{pv(t-1)} \\ \dots \\ P_{pv(t-p+1)} \\ DR(t-1) \dots DR(t-q+1) \end{array} \right] \\ \text{ref-fnn} \left[ \begin{array}{l} P_{pv(t2+td2)} \\ P_{pv(t2-td2-1)} \\ \dots \\ P_{pv(t2-td2-p+1)} \\ DR(t2-td2-1) \dots \\ DR(t2-td2-q+1) \end{array} \right] \\ \text{gnn} \left[ \begin{array}{l} P_{pv(t2-td2)} \\ P_{pv(t2-td2-1)} \\ \dots \\ P_{pv(t2-td2-p+1)} \\ DR(t2-td2-1) \\ \dots \\ DR(t2-td2-q+1) \end{array} \right] \end{array} \right\} \quad (11)$$

**DC-DC Boost Converter Model**

A boost converter is connected between the SPV generator and load. For effective controlling and to trace global maxima at PV curve there is an important variable of boost converter that is duty ratio [36-37]. Generally boost converter is considered ideal for the offline evaluation therefore its input power and power at output terminals are equal. Here only one boost converter has been proposed because it reduces the requirement of no of cells of SPV generator, switches, reduces switching loss, enhances efficiency, and is an economical solution.

Parameters of boost converter models are calculated by using Eq. (12) - (13):

$$\text{Inductance, } L = \frac{V_{ip} (V_{op} - V_{ip})}{f_{sw} \times I \times V_{op}} \quad (12)$$

$$\text{Capacitance, } C = \frac{I_{op} (V_{op} - V_{ip})}{f_{sw} \times V \times V_{op}} \quad (13)$$



Where  $V_{ip}$ ,  $V_{op}$  are inputs and output voltages in volt respectively and  $I_{op}$  is output current in amps.

$\Delta V, \Delta I$  are ripples in voltage and current respectively and  $f_{sw}$  is switching frequency.

### 5. Experimental Setup

PV solar module is selected in Matlab R2016a, and module design parameters of an array for well-supportive PV modules used in this paper are cross-verified by using two more softwares PVsyst 6.8.1 and SAM software developed by the national renewable energy laboratory (NREL)[28]. The database is selected according to the variable, unpredictable insolation, and temperature pattern exploring the potential of the proposed scheme for SPV generator. This model can be recreated for other well-supportive modules with a suitable rating of boost converter for other recorded databases in the same manner.

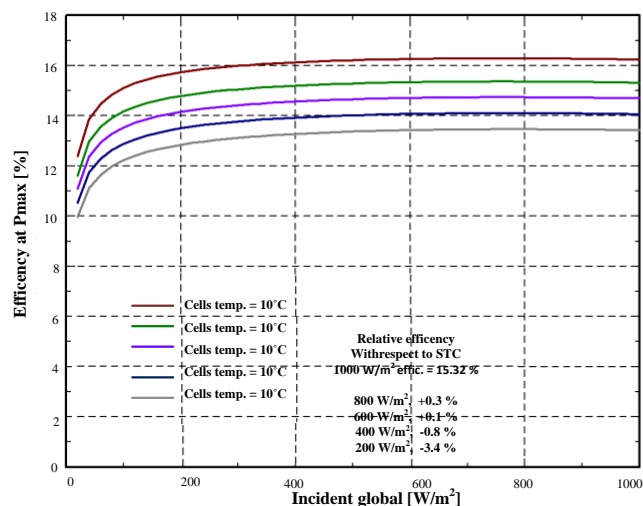


Fig.5(a) Efficiency-irradiation characteristics of the proposed system

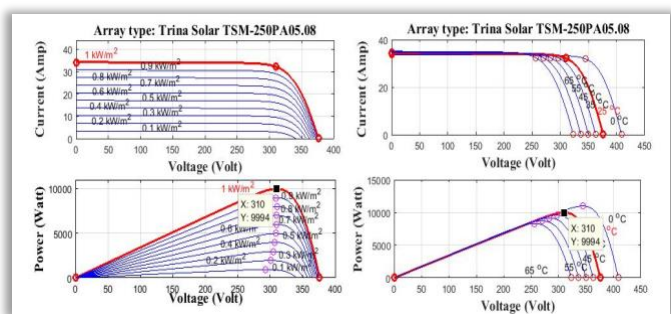


Fig.5(b) The IV and PV characteristics of the proposed system

The characteristics of efficiency-irradiation are shown in Fig.5(a). And the characteristics IV and PV of the proposed configuration under variable, unpredictable insolation, and temperature pattern are expressed in Fig.5(b). Parameters

description for one SPV generator module with their rated values used for the proposed technique is mentioned in Table 2.

Table 2. Parameters of one SPV generator module used are mentioned below

| PARAMETERS                     | VALUES OBTAINED |
|--------------------------------|-----------------|
| Maximum Power                  | 249.86 w        |
| Open Circuit Voltage, (Voc)    | 37.6 V          |
| Cells Per Module, (Ncell)      | 60 no.          |
| Short-Circuit Current, Isc     | 8.55 Amp        |
| Light Generated Current, $I_L$ | 8.5795 Amp      |

The key issues we have attempted to find the solution include-

1. Efficient controlling under nonlinearities and episodically uncertainties which are unavoidable issues.
2. Extracting power from SPV generator at maxima to increase the sustainability of SPV generator.
3. Obtaining power with dynamic environmental conditions varies according to the season for a long term over any area with less chattering.
4. Controlling two inputs of two SPV generators with one boost converter to make the system efficient in case of shedding conditions and supply continues power economically.

### Input Dataset

The controller is trained by using Levenberg-Marquardt standard algorithm. The author has used five sets of the database to prove the controlling efficiency of the controller to make SPV generator more justifiable as a famous source of renewable energy.

1. **Database-I-** This set is containing 10910 samples of variables presented by insolation pattern-I in Fig.6. The purpose of taking a large no of samples is to check the controlling proficiency of the controller in dynamic conditions. This is our aim to design a controller that can work efficiently on large environmental data which varies according to season over a large period worldwide.
2. **Database-II-** In this set author is using 246 samples indicated by insolation pattern-II in Fig.6. The purpose of taking 246 samples for the second case is to validate the controller's feasibility in any condition whether it is working for macro or micro-environmental data.

- Database-III-** In this set 100 samples are taken represented by the temperature dataset as shown in Fig.6. These samples consist of temperature data that affects the performance of the SPV generator.
- Database-IV-** In this set 31 samples are taken indicated by insolation pattern-IV in Fig.6. These samples consist of micro-environmental data with unpredictable weather changes during sunny days.
- Database-V-** In this set 981 samples are taken as mention in Fig.6 by insolation pattern-V. These samples consist of macro-environmental data with large variation of insolation pattern.

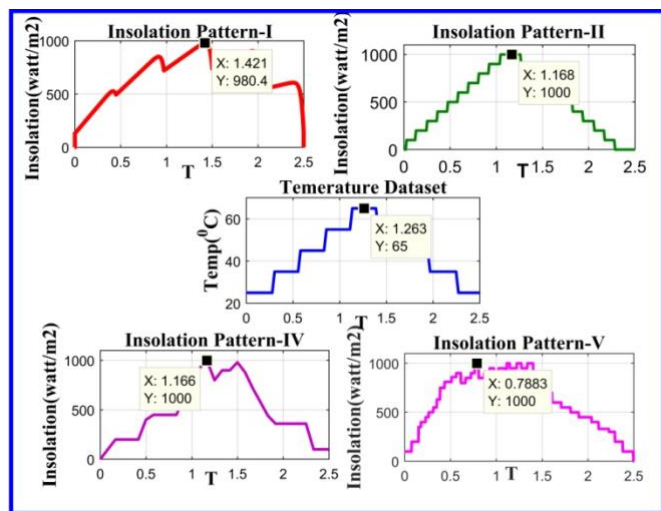


Fig.6 Database-I, Database-II, Database-III, Database-VI, and Database-V

## 6. Results and Discussion

Performance analysis of MPPT technique using MIASO based NARMA-L2 controller on SPV generator has been done. In this context post-processing performance assessment has been divided into two sections:

### 7.1. Part-I-

Here in this section the evaluation of the performance of MPPT technique using MIASO based NARMA-L2 controller of SPV generator is carried out through performance index.

- MSE (Mean Square Error)-** This is a minimization criteria. This is the error calculated as the difference between generated plant output and targeted response. This index is in terms of quantity to find the closeness of forecasts or predictions to get the desired outcome.

$$MSE = \frac{1}{n} \sum_{i=1}^n (\text{Desired\_output} - \text{plant\_output})^2 \tag{14}$$

Here n is number of data sample

- Mu-** This is a measure representing the compliance or learning rate of the network. If this is at the maximum value it means the learning rate has attained its maximum position and training. After reaching this value it will result in termination of validation.
- Gradient** – This shows the direction of alteration in values.

Table 3. Summary of Performance Index

|              |                |            |
|--------------|----------------|------------|
| Database-I   | No. of Samples | 10910      |
|              | MSE            | 7.4252e-07 |
|              | Mu             | 1e-09      |
| Database-II  | Gradient       | 6.873e-07  |
|              | No. of Samples | 246        |
|              | MSE            | 0.00310    |
| Database-III | Mu             | 1e-05      |
|              | Gradient       | 0.000173   |
|              | No. of Samples | 100        |
| Database-IV  | MSE            | 0.024867   |
|              | Mu             | 1e-10      |
|              | Gradient       | 3.83e-16   |
| Database-V   | No. of Samples | 31         |
|              | MSE            | 0.2033     |
|              | Mu             | 1e-09      |
|              | Gradient       | 4.4974e-14 |
| Database-VI  | No. of Samples | 981        |
|              | MSE            | 0.0011397  |
|              | Mu             | 1e-07      |
|              | Gradient       | 8.3689e-5  |

From Table 3. author found out that the MSE value is 7.4252e-07 for database-I which is less than the value 0.00310 , 0.024867, 0.2033 and 0.0011397 for database-II, database-III , database-IV and database-V respectively. It is indicating that accuracy is enhanced for a large number of training samples and that fulfills our aim. As a result of this controller can efficiently and precisely trace the desired output. And we got higher output under dynamic conditions.

### 7.2. Part –II-

Here in this section, the effectiveness of the proposed MPPT technique using MIASO based NARMA-L2 controller of SPV generator is demonstrated by simulation results, and simulation is carried out in MATLAB/Simulink. Fig.7 is showing a MATLAB model of the proposed SPV generator with MPPT technique using



MIASO based NARMA-L2 controller. This model is representing past data or present values as input and desired parameters. Here the input is desired reference. Two NARMA-L2 controllers are used for two SPV generators. Five data sets as shown in Fig.6 are used as inputs for the teaching process of these two controllers. Here time delay of 1.8 sec and 2 sec is created between two input signals of SPV generator and one output signal as the duty cycle is generated to extract power output at maxima.

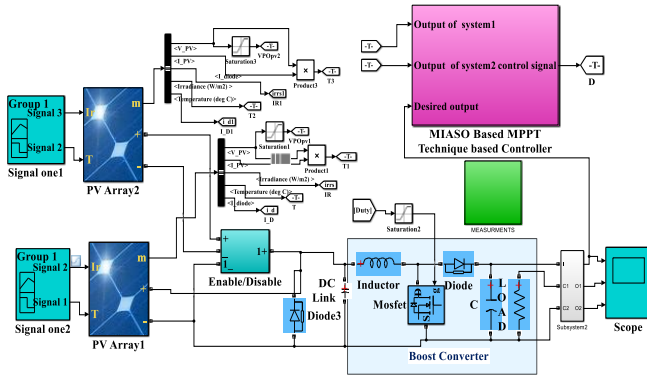


Fig.7 MATLAB modeling of the proposed technique for SPV generator

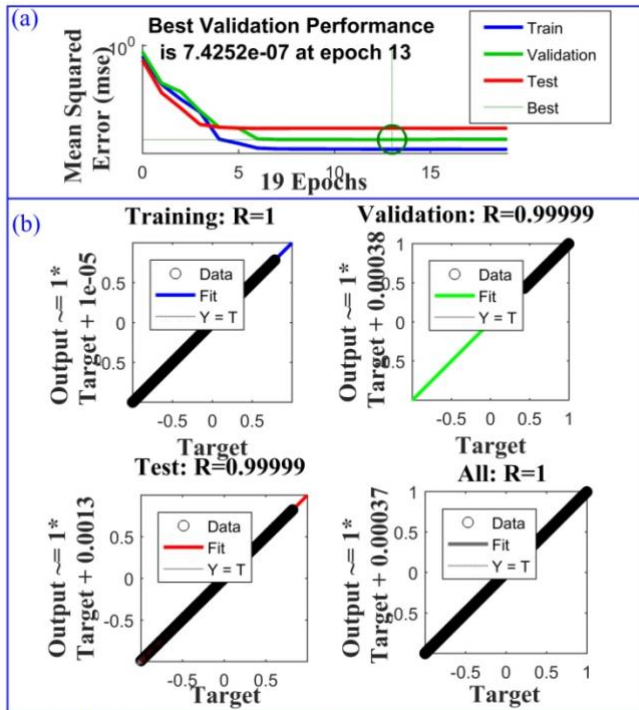


Fig.8 Performance of controller obtained after training for dataset-I

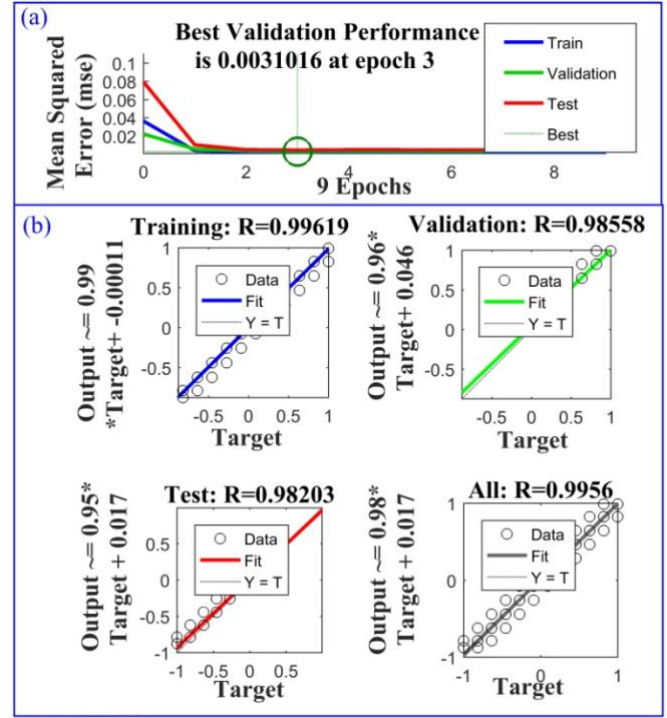


Fig.9 Performance of controller obtained after training for dataset-II

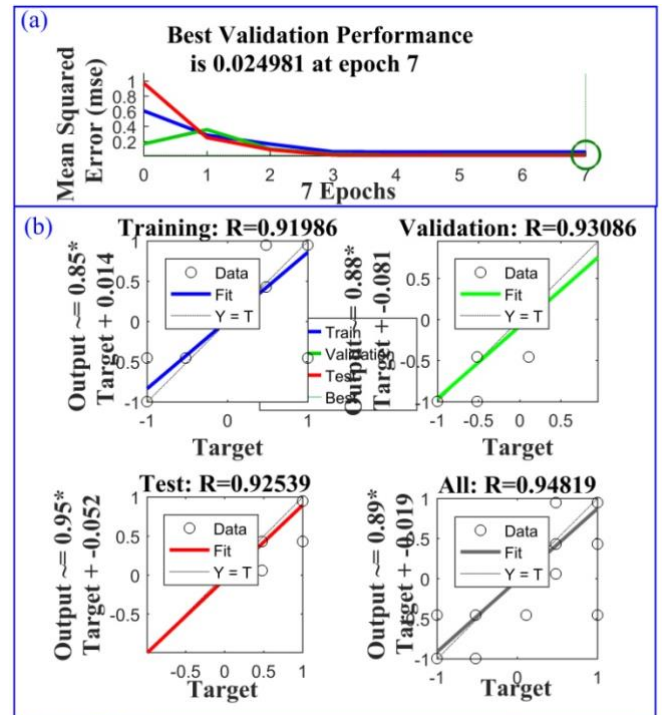


Fig.10 Performance of controller obtained after training for dataset-III

Performance of controller obtained after training is presented in Fig.8(a), Fig.9(a), Fig.10(a), Fig.11(a), and Fig.12(a) for dataset-I, dataset-II, dataset-III, dataset-IV and dataset-V respectively.

Figures 8(b), Fig.9(b), Fig.10(b), Fig.11(b), and Fig.12(b) are indicating the correlation between the input and output of the controller. One indicates the strong correlation for dataset-I in comparison to dataset-II, dataset-III, dataset-IV, and dataset-V. It proves how precisely output follows input and strongly indicates the best performance.

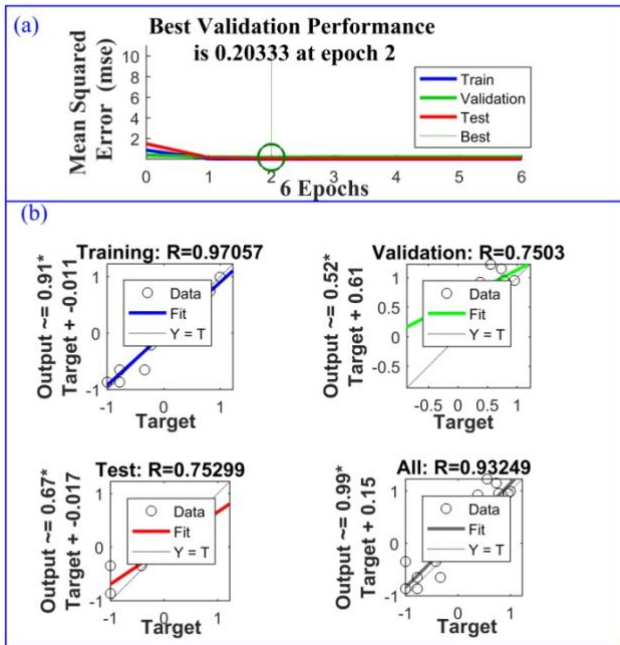


Fig.11 Performance of controller obtained after training for dataset-IV

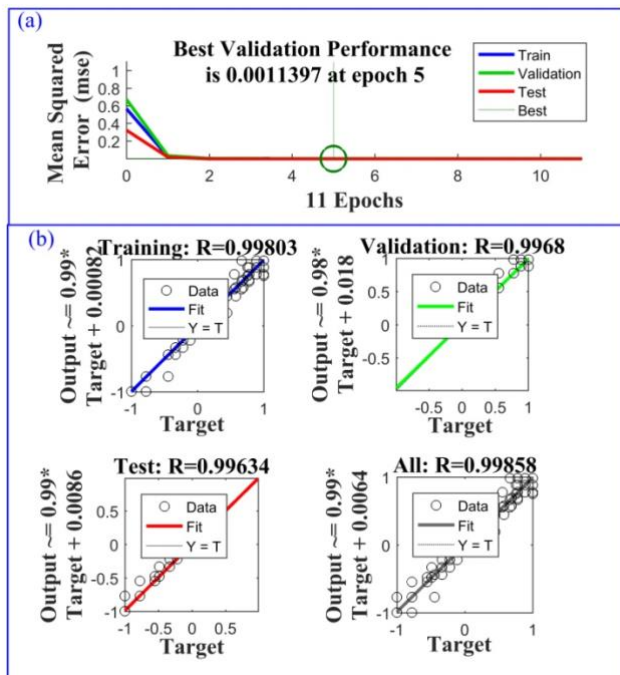


Fig.12 Performance of controller obtained after training for dataset-V

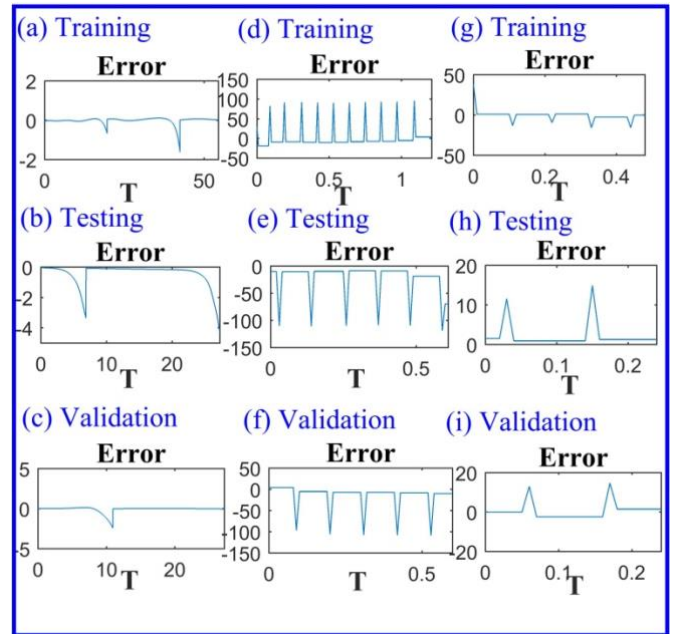


Fig.13 Errors during the training, testing, and validation process with databaset-I, databaset-II and databaset-III

Figure 13(a), Fig.13(b), Fig.13(c) represents the errors during the training, testing, and validation process with database-I, Fig.13(d), Fig.13(e), Fig.13(f) represents the errors during the training, testing, and validation process with database-II, Fig.13(g), Fig.13(h), Fig.13(i) represents the errors during training, testing and validation process with database-III.

Figure 14(a), Fig.14(b), Fig.14(c) represents the errors during training, testing and validation process with database-IV, and Fig.14(d), Fig.14(e), Fig.14(f) reports the errors during training, testing and validation process with database-V.

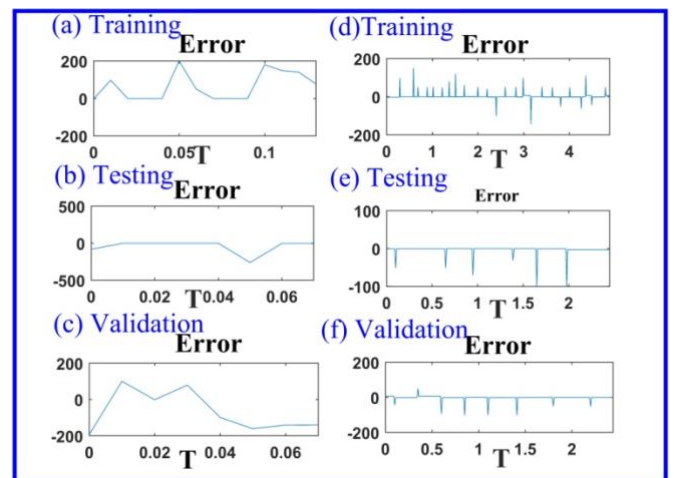
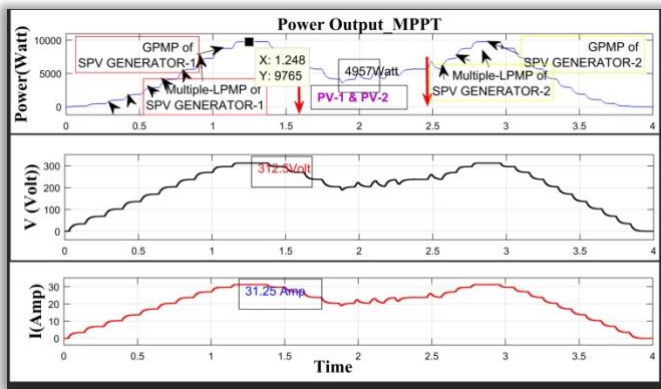


Fig.14 Errors during the training, testing, and validation process with databaset-IV and databaset-V

In Fig.15 proposed scheme is implemented on two SPV generators to control one boost converter for 246 samples which is a complex case of variation in insolation at different levels from 100 watt/m<sup>2</sup> to 1000 watt/m<sup>2</sup> at 25°C .

From Fig.15 the value of power obtained with the controller is 9765 watt at 1000 watt/m<sup>2</sup> insolation, 25°C. And the rated power is 9994 watt, at 1000 watt/m<sup>2</sup> insolation and 25°C. It illustrates that power conversion efficiency using the proposed technique is 97.70%. That enhances the SPV generator output at variable insolation patterns.

In addition, the proposed technique is controlling the output of both SPV generators at a 1.8 sec delay. From 1.8 sec to 2.5 sec, both SPV generators are working at low incident insolation 600 watt/m<sup>2</sup> or below. Power at low incident insolation of both connected SPV generators is 4957 watt which is proving that the controller is efficiently controlling both connected SPV generators.



**Fig.15** Power, Voltage and Current output with the proposed technique for dataset-I

Now at 2.5 sec SPV generator-1 is disconnected being out of order in this condition then SPV generator-2 will supply continuous power to the load and will provide maximum power 9765 watt at 1000 watt/m<sup>2</sup> insolation, 25°C. This proves that the proposed technique can control both SPV generator or one SPV generator if the second SPV generator is out of order or according to demand.

There is more than one LPMP as shown in the simulation result from Fig.15. The proposed controller is intelligent enough to differentiate between GPMP and LPMP. Thus SPV generator with the controller gives maximum power 9994 watt at 1000watt/m<sup>2</sup> power density.

This is the biggest argument that we have to check the controllability of the controller for large no of seasonal, weekly, monthly, and yearly worldwide environmental data. Therefore in Fig.17, the proposed scheme is implemented for 10910 samples to see the proposed technique’s performance on fast-changing and large no of samples at different levels of insolation. Here the author has

checked performance for fast-changing insolation that varies from 10.18 watt/m<sup>2</sup> to 980.46 watt/m<sup>2</sup> at 25°C.

The value of power obtained from simulation results is 9606 watts as shown in Fig.17 and the rated power of one SPV generator is 9787 watt at 980.46 watt/m<sup>2</sup> insolation, 25°C presented by Fig.16. It shows that power conversion efficiency using the proposed technique is 98.15%. Therefore it illustrates that the proposed technique is working more efficiently on large no of dynamic environment data.

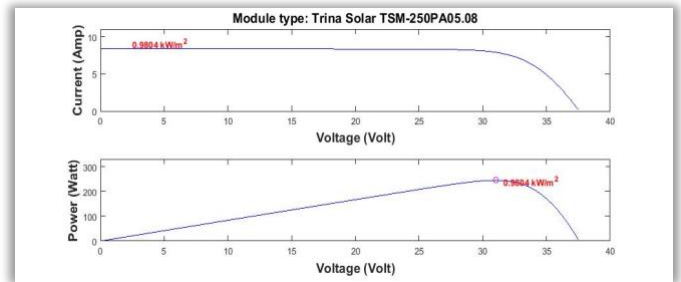


**Fig.16** Rated PV and VI curve

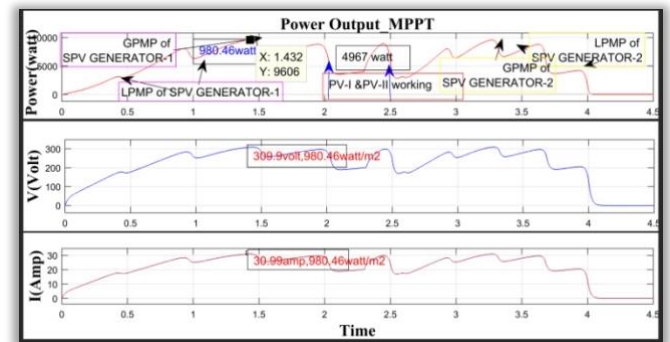


**Fig.17** Power, Voltage and Current output with the proposed technique for dataset-II

In addition, the proposed technique is controlling the output of both SPV generators at a 2 sec delay. From 2 sec to 2.5 sec, both SPV generators are working at insolation considered 600 watt/m<sup>2</sup> or below. The power extracted at low-level insolation of both connected SPV generators is 4967 watt as shown by Fig.17 which is demonstrating that the controller is efficiently controlling both connected SPV generators.

Now at 2.5 sec, SPV generator-1 is disconnected being out of order. And at this condition, the SPV generator-2 is supplying continuous optimum power i.e. 9606 watt at 980.46 watt/m<sup>2</sup> to the connected load. This is indicating that two SPV generators can supply power reliably according to the requirement of the connected load.

There is more than one LPMP as shown in Fig.17. The proposed controller is trained to differentiate GPMP and LPMP. Here the SPV generator-2 gives maximum power 9606 watt at the power density of 980.46 watt/m<sup>2</sup>.



In Fig.18 proposed scheme is implemented for 100 samples to see the proposed technique's performance on the variation of temperature.

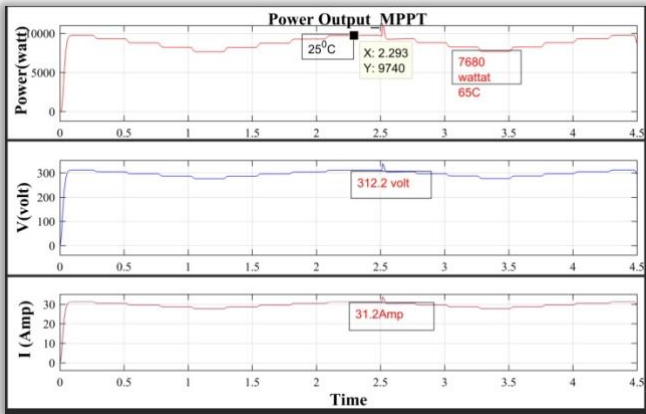


**Fig.18** Power, Voltage and Current output with the proposed technique for dataset-III

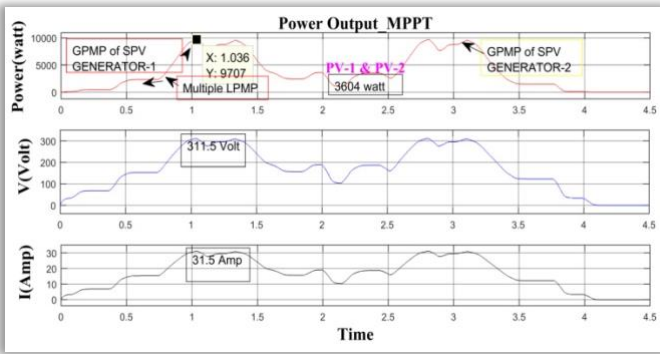


**Fig.19** Power, Voltage and Current output with the proposed technique for dataset-IV

The value of power is 9740 watt and the rated power is 9994 watt, at 1000 watt/m<sup>2</sup> insolation and 25°C It is expressing that power conversion efficiency using the proposed technique is 97.40%.

Here two more datasets are used to check controller's working in unpredictable condition. In Fig.19 proposed scheme is implemented for 31 samples as micro-environmental sample-II.

The value of power is 9707 watt and the rated power is 9994 watt, at 1000 watt/m<sup>2</sup> insolation and 25°C It is expressing that power conversion efficiency using the proposed technique is 97.12%.

In addition, the proposed technique is controlling the output of both SPV generators at a 2 sec delay. From 2 sec to 2.5 sec, both SPV generators are working at insolation considered 500 watt/m<sup>2</sup> or below. The power extracted at low-level insolation of both connected SPV generators is 3604 watt as shown by Fig.19 which is showing that the controller is efficiently controlling both connected SPV generators.

Now at 2.5 sec, SPV generator-1 is disconnected and at this condition, the SPV generator-2 two is supplying continuous optimum power i.e. 9707 watt at 1000 watt/m<sup>2</sup> to the connected load. This is indicating that two SPV generators can supply power reliably according to the requirement of the connected load.

There is more than one LPMP as shown in Fig.19. The proposed controller is trained to differentiate GPMP and LPMP. Here the SPV generator-2 gives maximum power 9707 watt at the power density of 1000 watt/m<sup>2</sup>.

In Fig.20 proposed scheme is implemented for 981 samples as macro-environmental sample. The value of power is 9755 watt and the rated power is 9994 watt, at 1000 watt/m<sup>2</sup> insolation and 25°C It is expressing that power conversion efficiency using the proposed technique is 97.60%.

In addition, the proposed technique is controlling the output of both SPV generators at a 2 sec delay. From 2 sec to 2.5 sec, both SPV generators are working at insolation considered 500 watt/m<sup>2</sup> or below. The power extracted at low-level insolation of both connected SPV generators is 1745 watt as shown by Fig.20 which proves that the controller is efficiently controlling both connected SPV generators.

Now at 2.5 sec, SPV generator-1 is disconnected and at this condition, the SPV generator-2 is supplying continuous optimum power i.e. 9755 watt at 1000 watt/m<sup>2</sup> to the connected load. This is indicating that two SPV generators can supply power reliably according to the requirement of the connected load.

There is more than one LPMP as shown in Fig.20. The proposed controller is trained to differentiate GPMP and LPMP. Here the SPV generator-2 gives maximum power 9755 watt at the power density of 1000 watt/m<sup>2</sup>. Therefore we found that for five different datasets proposed scheme has proved its better performance.

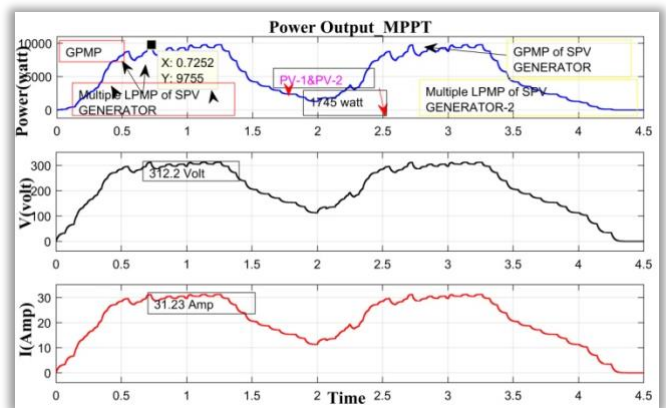


**Fig.20** Power, Voltage and Current output with the proposed technique for dataset-V

**Table 4.** Performance Summary of Proposed Technique

|             | Nature of Samples                 | Power Output_Rated                              | Power Output_MPPT | Efficiency_MPPT |
|-------------|-----------------------------------|---|-------------------|-----------------|
| Dataset-I   | Fast-Changing/<br>Dynamic Samples | 9787 watt at 980.40 watt/m <sup>2</sup> , 25 °C | 9606 watt         | 98.15 %         |
| Dataset-II  | Micro-environmental Samples-I     | 9994 watt at 1000 watt/m <sup>2</sup> , 25 °C   | 9765 watt         | 97.70 %         |
| Dataset-III | Temperature Samples               | 9994 watt at 1000 watt/m <sup>2</sup> , 25 °C   | 9740 watt         | 97.40 %         |
| Dataset-IV  | Micro-environmental Samples-II    | 9994 watt at 1000 watt/m <sup>2</sup> , 25 °C   | 9707 watt         | 97.12%          |
| Dataset-V   | Macro-environmental Samples       | 9994 watt at 1000 watt/m <sup>2</sup> , 25 °C   | 9755 watt         | 97.60 %         |

**7. Conclusion**

The most important achievement of this paper is the improved performance of the proposed novel MPPT technique using MIASO based NARMA-L2 controller for two SPV generators with one boost converter in finding a point of maximum power on macro and micro-dynamic environmental data. The system simulation offers the least MSE 7.4252e-07, 0.024867, 0.00310, 0.2033 and 0.0011397 for the large number of samples 10910, 246, 100, 31 and 981 respectively. This proves that it can control the output precisely to get desired output, for macro as well as micro-environmental data. From the simulation results, it is proved that the controller works excellently with one SPV generator or both simultaneously. Therefore SPV generator can supply power continuously to the connected load if one source gets disconnected being out of order. In addition, it is found that the power tracking efficiency of the proposed MPPT technique is 98.15% for large no of dynamic weather data, and 97.70%, 97.40% 97.12%, 97.60% efficiency for 246 samples,100 samples, 31 samples, 981 samples of weather data respectively. It indicates that the proposed technique enhances the performance of both SPV generators on macro and micro-weather data over a long period and as well as for seasonal variations. Also, it is proved that the proposed technique is intelligent enough to differentiate GPMP and LPMP on complex nonlinear PV curves as it is supplying power at

maxima. Two SPV generators with one boost converter provide the best economic solution and both SPV generator's capacities can control according to demand. Finally, it is established that the proposed methodology optimizes the performance of SPV generators to accept it as a more promising renewable energy source.

**Reference:**

- [1]. United Nations, "The Sustainable Development Goals Report 2020", pp.66, 2020. (Standards and Reports)
- [2]. O. Kaplan, U. Yavanoglu and F. Issi, "Country Study on Renewable Energy Sources in Turkey", International Conference on Renewable Energy Research and Applications (ICRERA), pp.1-5, 2012. (Conference Paper)
- [3]. Global Energy Statistical Year Book 2020. <https://yearbook.enerdata.net/total-energy/world-consumption-statistics.html>. (Standards and Reports)
- [4]. F. Ayadi, I. Colak, I. Garip and H. I. Bulbul, "Impacts of Renewable Energy Resources in Smart Grid," 2020 8th International Conference on Smart Grid icSmartGrid, pp. 183-188, 2020. (Conference Paper)
- [5]. Kenneth E. Okedu, A. Al Senaidi, I. Al Hajri, I. Al Rashdi and W. Al Salmani., "Real-Time Dynamic Analysis of Solar PV Integration for Energy Optimization", International Journal of Smart Grid – ijSmartGrid , Vol.4, No.2, 2020. (Article)
- [6]. Tanveer Ahmad and Dongdong Zhang, "A Critical Review of Comparative Global Historical Energy Consumption and Future Demand: The Story told so Far", Energy Reports, Vol.6, pp.1973-1991, 2020. (Article)
- [7]. Shahd Fadhil Jaber and Amina Mahmoud Shakir, " Design and Simulation of a Boost-microinverter for Optimized Photovoltaic system Performance", International Journal of Smart Grid – ijSmartGrid, Vol.5, No.2, 2021. (Article)
- [8]. PVSYST6.8.1 software, www.Pvsyst.Com. Accessed 22 July 2021 [Online].
- [9]. Ali Omar Baba, Guangyu Liu and Xiaohui Chen, "Classification and Evaluation Review of Maximum Power Point Tracking Methods", Sustainable Futures, Vol.2, 2020. (Article)
- [10]. D. Gueye, Mahamadou Abdou Tankari, D. Gueye and Alp Housseyni Ndiay, "Design Methodology of Novel PID for Efficient Integration of PV Power to Electrical Distributed Network", International Journal of Smart Grid – ijSmartGrid, Vol.2, No.1, 2018. (Article)
- [11]. Abdelhakim Belkaid, Ilhami Colak, Korhan Kayisli, and Ramazan Bayindir, "Design and Implementation of a Cuk Converter Controlled by a Direct Duty Cycle INC-MPPT in PV Battery System", International Journal of Smart Grid – ijSmartGrid, Vol.3, No.1, 2019. (Article)
- [12]. M. Premkumar, C. Kumar, R. Sowmya and J. Pradeep, "A Novel Salp Swarm Assisted Hybrid Maximum Power Point Tracking Algorithm for The Solar Photovoltaic Power Generation systems", Automatika, Vol.62, pp.1-20, 2020. (Article)

- [13]. Belkaid, I. Colak, K. Kayisli and R. Bayindir, "Improving PV System Performance using High Efficiency Fuzzy Logic Control", 2020 8th International Conference on Smart Grid (icSmartGrid), 2020, pp. 152-156, 2020. (Conference Paper)
- [14]. Aman Ismael Nusaif and Anas Lateef Mahmood, "MPPT Algorithms (PSO, FA, and MFA) for PV System Under Partial Shading Condition, Case Study: BTS in Algalazia, Baghdad", International Journal of Smart Grid – ijSmartGrid, Vol.10, No.3, 2020. (Article)
- [15]. S. Ryvkin and F. Himmelstoss, "Two controls of novel buck-boost converter for solar photovoltaics," 2012 International Conference on Renewable Energy Research and Applications (ICRERA), pp. 1-6, 2012. (Conference Paper)
- [16]. F. Li, M. Alshareef, Z. Lin and W. Jiang, "A modified MPPT algorithm with integrated active power control for PV-battery systems," 2016 IEEE International Conference on Renewable Energy Research and Applications (ICRERA), pp. 742-746, 2016. (Conference Paper)
- [17]. K. S. Rajesh, S. S. Dash, Bayinder, R. Sridhar and R. Rajagopal, "Implementation of an adaptive control strategy for solar photo voltaic generators in microgrids with MPPT and energy storage," 2016 IEEE International Conference on Renewable Energy Research and Applications (ICRERA), pp. 766-771, 2016. (Conference Paper)
- [18]. Tao Ma, Hongxing Yang and Lin Lu, "Solar Photovoltaic System Modeling and Performance Prediction", Renewable and Sustainable Energy Reviews, Vol.36, pp.304-315, 2014. (Article)
- [19]. P. Meena, S. Gautam, and S. Chahar, "Solar PV Based Grid Interfaced System with Power Quality Improvement", 2019 2nd International Conference on Power Energy, Environment and Intelligent Control (PEEIC), pp.543-546, 2019. (Conference Paper)
- [20]. B. Subudhi and R. Pradhan, "A Comparative Study on Maximum Power Point Tracking Techniques for Photovoltaic Power Systems", in IEEE Transactions on Sustainable Energy, Vol. 4, No. 1, pp. 89-98, Jan. 2013. (Article)
- [21]. Ratnakar Babu Bollipo, Suresh Mikkili and Praveen Kumar Bonthagorla, "Critical Review on PV MPPT Techniques: Classical, Intelligent and Optimisation", IET Renew. Power Gener., Vol. 14 Iss. 9, 2020.ref21 (Article)
- [22]. S. Bhattacharyya, D. S. Kumar P, S. Samanta and S. Mishra, "Steady Output and Fast Tracking MPPT (SOFT-MPPT) for P&O and InC Algorithms", in IEEE Transactions on Sustainable Energy, Vol.12, No.1, pp. 293-302, 2021. (Article)
- [23]. Yadav A.K. and Malik H., "ANN and Multiple Linear Regression-Based Modelling for Experimental Investigation of Photovoltaic Module Maximum Power Production Under Outdoor Condition of Mountainous Region", In: Eltamaly A., Abdelaziz A. (eds) Modern Maximum Power Point Tracking Techniques for Photovoltaic Energy Systems. Green Energy and Technology. Springer, Cham. pp.229-245, 2019. (Article)
- [24]. Sufyan Samara and Emad Natsheh, "Modeling The Output Power of Heterogeneous Photovoltaic Panels Based on Artificial Neural Networks Using Low-cost Microcontrollers", Heliyon, Vol.4, Issue 11, 2018. (Article)
- [25]. Vishank Bhatia, V. Kalaichelvi and R. Karthikeyan, "Comparison of GA Tuned Fuzzy Logic and NARMA-L2 Controllers for Motion Control in 5-DOF Robot", International Journal of Computers and Applications, Vol.39, No.2, pp. 69-78, 2017. (Article)
- [26]. Md. Rashidul Islam, Jakir Hasan, Md. Mahmudul Hasan, Md. Najmul Huda, Mohammad Ashraf Hossain Sadi and Ahmed Abu Hussein, "Performance improvement of DFIG-based wind farms using NARMA-L2 controlled bridge-type flux coupling non-superconducting fault current limiter", in IET Generation, Transmission & Distribution, Vol.14, pp. 6580 – 6593, Issue 26, 2020 (Article)
- [27]. Mohamed Hallouz, Nadir Kabache, Samir Moulahoum, and Selman Kouadria, "Neural Network Based Field Oriented Control for Doubly-Fed Induction Generator", International Journal of Smart Grid – ijSmartGrid, Vol.2, No.3, 2018. (Article)
- [28]. H. Abu-Rub, A. Iqbal, S. M. Ahmed, F. Z. Peng, Y. Li, and G. Baoming, "Quasi-Z-Source Inverter-based Photovoltaic Generation System with Maximum Power Tracking Control Using ANFIS", IEEE Trans. Sustain. Energy, Vol.4, No.1, pp.11–20, 2013. (Article)
- [29]. R. M. Ahmed, N. E. Zakzouk, M. I. Abdalkader, and A. K. Abdelsalam, "Modified Partial-Shading-Tolerant Multi-Input-Single-Output Photovoltaic String Converter", in IEEE Access, Vol.9, pp.30663-30676, 2021. (Article)
- [30]. V. Kamaraj, N. Chellammal, B. Chokkalingam, and J.L. Munda, "Minimization of Cross-Regulation in PV and Battery Connected Multi-Input Multi-Output DC to DC Converter", Energies, Vol.13, No.24, 2020. (Article)
- [31]. C. Balaji, S. S. Dash, N. Hari, and P. C. Babu, "A Four-Port Non-Isolated Multi-Input Single Output DC-DC Converter Fed Induction Motor", 2017 IEEE 6th International Conference on Renewable Energy Research and Applications (ICRERA), pp.631-637, 2017. (Conference Paper)
- [32]. Ali M. Humada, Salih Y. Darweesh, Khalid G. Mohammed, Mohammed Kamile, Samen F. Mohammed, Naseer K. Kasim, Tahseen Ahmad Tahseen, Omar I. Awad, and Saad Mekhilef, "Modeling of PV System and Parameter Extraction Based on Experimental Data: Review and Investigation", Solar Energy, Vol.199, pp.742–760, 2020. (Article)
- [33]. N. A. Jalil and I. Z. M. Darus, "NARMA-L2 Vibration Controller for Flexible Structure with Non-Collocated Sensor-Actuator", Fifth International Conference on Computational Intelligence, Modelling and Simulation, pp.17-22. 2013. (Conference Paper)
- [34]. Y. Chen and H. Zhou, "Neural Network Control Approach of a Midwater Trawl System Based on Feedback Linearization", Proceedings of 2011 International Conference on Fluid Power and



- Mechatronics, pp.138-143, 2011. (Conference Paper)
- [35]. E Mukhin, V Tarasov and A Varchenko, "Bethe Eigenvectors of Higher Transfer Matrices", Journal of Statistical Mechanics Theory and Experiment, Vol.2006, pp.P08002-P08002, 2006. (Article)
- [36]. Saleh E. Babaa, Georges El Murr, Faisal Mohamed and Srilatha Pamuri, "Overview of Boost Converters for Photovoltaic Systems". Journal of Power and Energy Engineering, Vol.06, pp.16-31, 2018. (Article)